

Supporting Information

Flexible, transparent and high dielectric constant fluoropolymer-based nanocomposites with fluorides-constructed interfacial structure

*Li Li, Rui Feng, Yang Zhang and Lijie Dong**

Center for Smart Materials and Devices
Wuhan University of Technology, Wuhan 430070 P.R. China
Tel: (+86) 27-87651775 Fax: (+86)27-87651779
E-mail: dong@whut.edu.cn

Table of Contents

Experimental sections	3
Materials	3
Synthesis of POTS-modified SiO₂ nanoparticles (SPNs)	3
Fabrication of pure P(VDF-HFP) and P(VDF-HFP)/SPNs nanocomposite films	3
Characterization of SPNs	4
Characterization of P(VDF-HFP)/SPNs nanocomposite films	5
Results and Discussion	8
Reference	13

Experimental Sections

Materials: Poly(vinylidene fluoride-*co*-hexafluoropropylene) (P(VDF-HFP)) (10 mol% HFP) pellets were procured from Solvay Plastics. 1H,1H,2H,2H-perfluorooctyltriethoxysilane (POTS) was purchased from Alfa Aesar. Tetramethyl orthosilicate (TMOS) was purchased from Aladdin. N, N-dimethylformamide (DMF), aqueous ammonia, acetic acid and ethanol were all bought from Sinopharm Chemical Reagent Co., Ltd., China. All chemicals were used as received.

Synthesis of POTS-modified SiO₂ nanoparticles (SPNs): The synthesis method was according to a literature with some modifications.¹ Specifically, 0.2 mmol aqueous ammonia and 40 mL distilled water were mixed into a 250 mL flask and heated to 30°C, then 2.15 mmol TMOS was added into the solution drop by drop in 2 mins. The resultant solution was kept heated at 30 °C and vigorously stirred for 1 h. Following that, 0.42 mmol POTS dissolved in 2 mL ethanol was added in drop by drop in 2 mins. After that, the solution was kept heated at 30 °C and stirred for 24 h. Then, the solution was heated up to 80 °C, kept stirred for another 24 h to condense the modifier. In the next step, after cooled to room temperature, the solution was transferred into a dialysis bag (Pierce, molecular weight cut off 10000) to be dialyzed in the dialysis solution (a mixture of distilled water, ethanol, and acetic acid with the volume ratio 1:1:0.007) for 24 h. This procedure was repeated for five times. Then, the solution was totally frozen by liquid nitrogen and quickly put in a vacuum freeze drier for 24 h with condensing temperature at -58.3 °C and vacuum degree at 2.3 Pa. By this method, the SiO₂ nanoparticles modified by POTS (designed as SPNs) can be easily collected after the sublimation of water and ethanol.

Fabrication of pure P(VDF-HFP) and P(VDF-HFP)/SPNs nanocomposite films: SPNs with five different mass concentrations (1 wt.%, 5 wt.%, 10 wt.%, 15 wt.%, 20 wt.%) were incorporated into P(VDF-HFP) matrix to form P(VDF-HFP)/SPNs nanocomposite films by a solution-casting method. Specifically,

150 mg of P(VDF-HFP) pellets were totally dissolved in 3 mL DMF via ultra-sonication and oscillation processing without break. Following that, SPNs was added into the solution of P(VDF-HFP) and easily dispersed in the solution through ultra-sonication and oscillation. In the next step, the mixed solution was casted slowly and evenly on a flat and cleaned glass substrate, then dried at 60 °C for 12 h to evaporate the most solvent to obtain nanocomposite film. After that, the film was put inside a vacuum oven at 120 °C for 24 h to get rid of the residue solvent. The pure P(VDF-HFP) film and other P(VDF-HFP)/SPNs nanocomposite films with SPNs contents of 5 wt.%, 10 wt.%, 15 wt.% and 20 wt.% were fabricated through the same procedures. After being stripped from the substrate, the pure P(VDF-HFP) and P(VDF-HFP)/SPNs nanocomposite films were obtained with 15~20 μm in thickness as measured.

Characterization of SPNs: Field emission transmission electron microscope (FETEM) images were taken to display the morphology and sizes of SPNs using a Joel JEM-2100F instrument. Samples of SPNs for TEM measurement were prepared by depositing a drop of ethanol solution dispersed with SPNs on the carbon coated copper grids, followed by air-drying. The subsidiary Energy Dispersive Spectrometer (EDS) to FETEM was used to show the elements composition of SPNs. X-ray photoelectron spectroscopy (XPS) was also used to figure out the elements composition as well as chemical states with an ESCALAB 250Xi from Thermo Fisher Co., Ltd. To characterize and analyze the chemical structure of SPNs, a Fourier transform infrared (FTIR) spectrometer (Nicolet 6700) was further employed to record the vibration spectra of SPNs. The spectra were measured at room temperature over a range of 4000-400 cm^{-1} , with a resolution of 1 cm^{-1} . The thermal properties of SPNs were characterized by using a thermogravimetric analysis (TGA) instrument (STA449F3) at a heating rate of 10 °C/min from 50 °C to 800 °C under nitrogen atmosphere.

Characterization of P(VDF-HFP)/SPNs nanocomposite films: TEM was also used to show the dispersion of SPNs in P(VDF-HFP) matrix using a Tecnai G20 TWIN instrument. Samples of P(VDF-HFP)/SPNs nanocomposite films for TEM measurement were prepared by cutting an ultrathin sections of nanocomposite films previously embedded in epoxy. To characterize the chemical structures and crystallization behaviors of pure P(VDF-HFP) and P(VDF-HFP)/SPNs nanocomposites, Fourier transform infrared (FTIR), X-ray diffraction (XRD) and differential scanning calorimetry (DSC) were employed. A Nicolet 6700 Fourier transform infrared spectrometer from Thermo Nicolet Co., Ltd. was also used to record the vibration spectra of pure P(VDF-HFP) and P(VDF-HFP)/SPNs nanocomposites and analyze the composition of crystalline phases of P(VDF-HFP). The spectra were measured at room temperature over a range of 4000-400 cm^{-1} , with a resolution of 1 cm^{-1} . According to the Lambert-Beer law, the relative fractions of TTTT conformation, corresponding to β -phase of P(VDF-HFP), can be derived from the FTIR spectra based on the specific absorption bands of α -phase and β -phase, using the following equation:²

$$F(\beta) = \frac{A_{\beta}}{\left(\frac{K_{\beta}}{K_{\alpha}}\right)A_{\alpha} + A_{\beta}} \quad (1)$$

Where A_{α} and A_{β} are the absorbance of α -phase and β -phase at 764 cm^{-1} and 840 cm^{-1} , respectively. K_{α} ($6.1 \times 10^4 \text{ cm}^2 \text{ mol}^{-1}$) and K_{β} ($7.7 \times 10^4 \text{ cm}^2 \text{ mol}^{-1}$) are the absorption coefficients at their respective wavenumbers.

A PYRIS1 DSC instrument from Perkin Elmer corporation was used to determine the crystallinity and analyze the crystallization behaviors of pure P(VDF-HFP) and P(VDF-HFP)/SPNs nanocomposite films. All film samples were heated from 30 $^{\circ}\text{C}$ to 200 $^{\circ}\text{C}$ at a rate of 10 $^{\circ}\text{C}/\text{min}$ under nitrogen atmosphere. After holding at the state for 5 min to eliminate the thermal history, the samples were cooled down to 30 $^{\circ}\text{C}$ at a rate of 10 $^{\circ}\text{C}/\text{min}$ and heated again from 30 to 200 $^{\circ}\text{C}$ at a rate of 10 $^{\circ}\text{C}/\text{min}$. The mass crystallinity (X_c) of P(VDF-HFP) was calculated via the following expression:³

$$X_c = \frac{\Delta H_m}{\Delta H_0} \times 100\% \quad (2)$$

where ΔH_m is the enthalpy of fusion derived from DSC melting curves and the weight of film samples, and ΔH_0 is the heat of fusion of 100% crystalline P(VDF-HFP), which is reported to be 104.7 J/g.⁴

XRD patterns of pure P(VDF-HFP) and nanocomposites were recorded using an X-ray diffractometer (D8 Advance) from Bruker Ltd. with Cu-K ($\lambda=1.5418 \text{ \AA}$) radiation. The scanning angle was from 10° to 30° with a scanning rate of $2^\circ/\text{min}$ at room temperature. To study the influence of SPNs on the crystallization behaviors of P(VDF-HFP) polymer, the average crystallite size L was calculated via the Scherer formula:⁵

$$L = \frac{K\lambda}{\beta \cos \theta} \quad (3)$$

where K is a dimensionless shape factor, generally equal to 0.89, $\lambda=1.5418 \text{ \AA}$ (Cu- K_α), β is the line broadening at half the maximum intensity (FWHM) and θ is the Bragg diffraction angle. The contents of crystalline phases and amorphous phases of P(VDF-HFP) were derived following the formula:

$$B = \frac{A}{A'} \times 100\% \quad (4)$$

where B is the phase ratio, A is the area of crystalline or amorphous peaks and A' is the total area of diffraction patterns. All the calculations are based on the Gaussian-Lorentz superposition fitting functions using Jade software.

The thermal properties of P(VDF-HFP)/SPNs nanocomposite films were characterized by using a thermogravimetric analysis (TGA) instrument (STA449F3) at a heating rate of $10^\circ\text{C}/\text{min}$ from 50°C to 900°C under nitrogen atmosphere.

Dielectric properties of pure P(VDF-HFP) and P(VDF-HFP)/SPNs nanocomposite films were investigated by using a precise digital LCR meter (E4980A, Agilent Ltd.) with frequency ranging from 20 Hz to 2 MHz at room temperature. The dielectric constant was calculated by the following equations:

$$\varepsilon = \frac{Cd}{\varepsilon_0 S} \quad (5)$$

where ε is the dielectric constant of the film samples, and C, d, S are the capacitance, thickness, effective area of the film samples, respectively. ε_0 is the free space permittivity, 8.854×10^{-12} F/m. Temperature dependent dielectric properties were conducted using a precise digital LCR meter (E4980A, Agilent Ltd.) and a heating furnace at a heating rate of 2 °C/min from 30 °C to 100 °C under a constant frequency of 1 kHz. High-field electric displacement against electric field (D-E) loops were measured at 10 Hz, under room temperature using a Mutiferroic-100V from Radient Technologies, Inc.

Light transmission tests of pure P(VDF-HFP) and P(VDF-HFP)/SPNs nanocomposite films were conducted using an Ultraviolet-Visible-Near Infrared (UV/VIS/NIR) Spectrometer (Lambda 750 S) from PerkinElmer Ltd. The mechanical properties of pure P(VDF-HFP) and P(VDF-HFP)/SPNs nanocomposite films were investigated through an equal-speed tension test on a microcomputer controlled electro-hydraulic servo universal testing machine (Instron1341) from Instron Ltd.

Results and Discussion

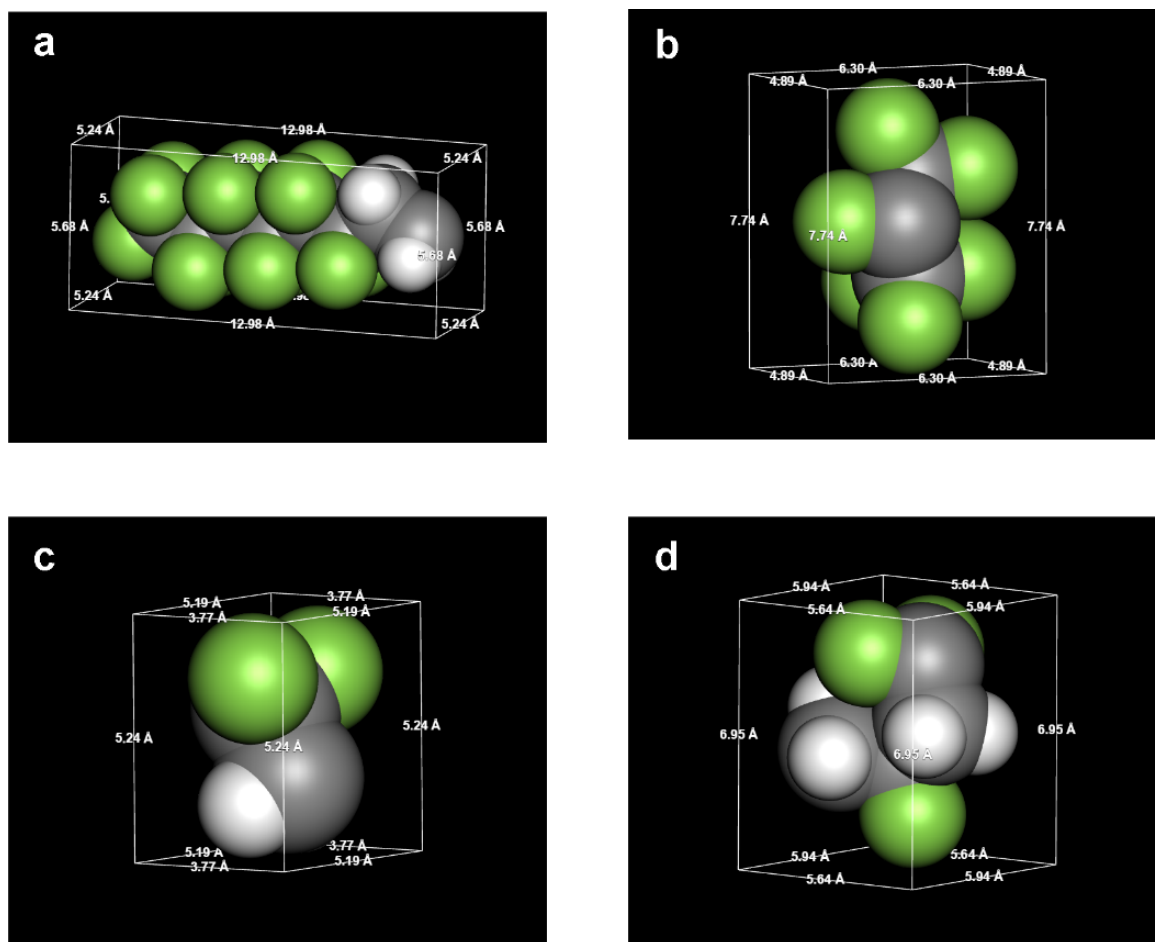


Figure S1. 3D models of a) fluorine group and minimum molecular units of b) HFP, c) TTTT conformation and d) TGTG' conformation. Blue, grey and white balls represent fluorine, carbon and hydrogen atoms, respectively. Models in b, c, d are constructed by selecting the typical segments of a long P(VDF-HFP) chain. The atom positions for calculating the sizes of every molecular model were all determined using Materials Studio software.

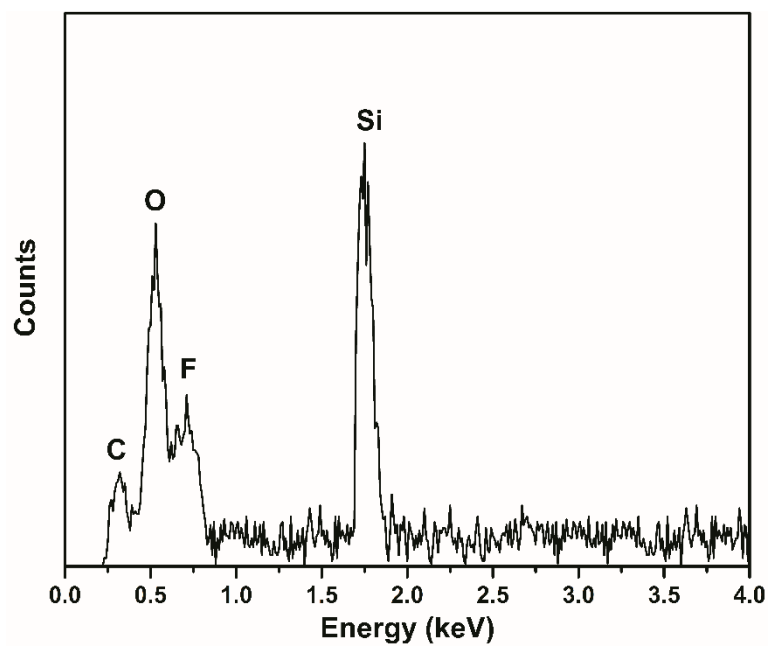


Figure S2. EDS spectrum of SPNs.

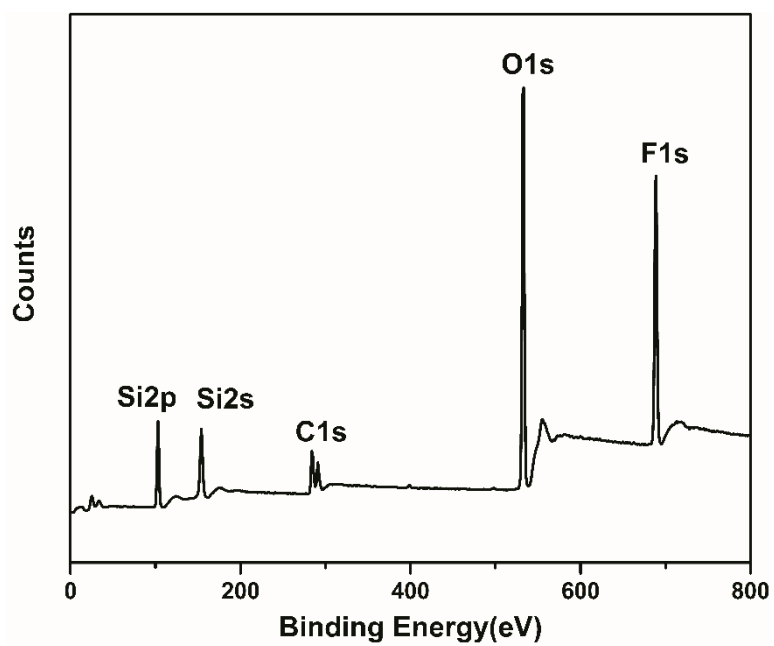


Figure S3. XPS spectrum of SPNs.

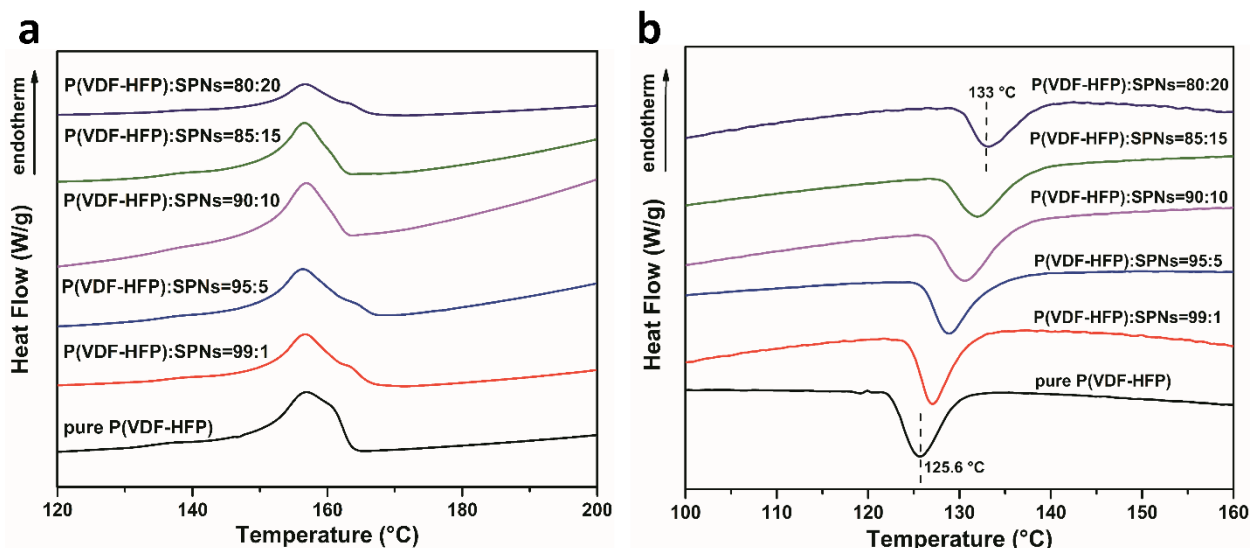


Figure S4. DSC thermograms of pure P(VDF-HFP) and P(VDF-HFP)/SPNs nanocomposite films with different SPNs contents during the a) heating cycle and b) cooling cycle.

Table S1. Crystallization temperature, melting temperature and crystallinity of pure P(VDF-HFP) and P(VDF-HFP)/SPNs nanocomposite films derived from DSC results.

Sample	T_c (°C)	T_m (°C)	Crystallinity (%)
Pure P(VDF-HFP)	125.6	156.8	26.72
P(VDF-HFP): SPNs=99:1	127.2	156.7	20.45
P(VDF-HFP): SPNs=95:5	128.8	156.6	19.08
P(VDF-HFP): SPNs=90:10	131.5	156.9	16.58
P(VDF-HFP): SPNs=85:15	132	156.8	16.01
P(VDF-HFP): SPNs=80:20	133.2	156.8	14.54

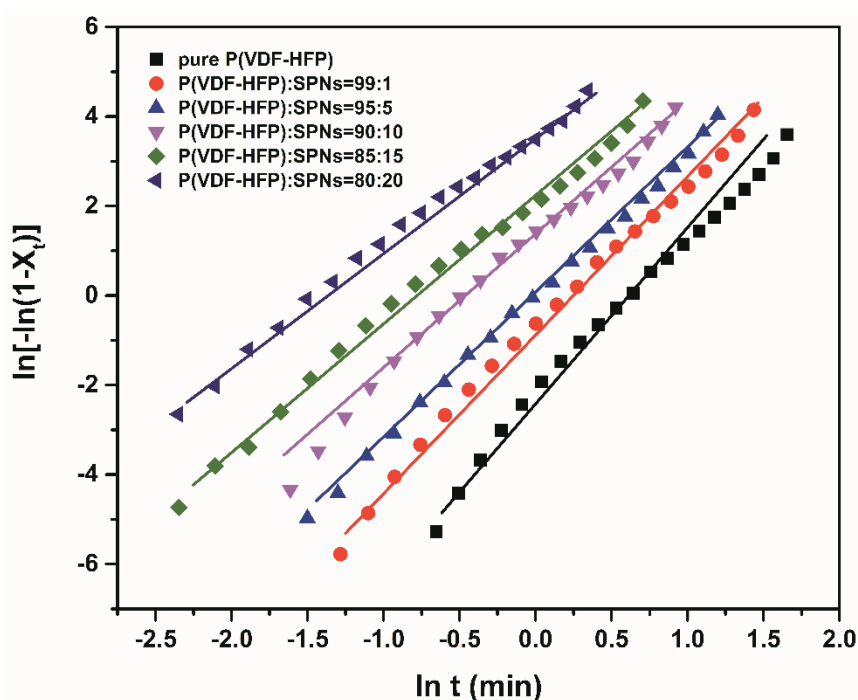


Figure. S5 Avrami plots $\ln [-\ln(1-X_t)]$ against $\ln t$ of pure P(VDF-HFP) and P(VDF-HFP)/SPNs nanocomposites with different contents of SPNs. $\ln [-\ln(1-X_t)] = \ln K + n \ln t$, Where X_t is the temperature-dependent relative crystallinity, t is the duration of the crystallization, K is the constant of crystallization rate and n is the Ozawa exponent.⁶

Table. S2 Values of n , k and $t_{1/2}$ for pure P(VDF-HFP) and P(VDF-HFP)/SPNs nanocomposites with different contents of SPNs, derived from Avrami plots.

Sample	n	K	$t_{1/2}$ (min)
Pure P(VDF-HFP)	3.571	0.00091	0.782
P(VDF-HFP): SPNs=99:1	3.448	0.00673	0.724
P(VDF-HFP): SPNs=95:5	3.210	0.01831	0.644
P(VDF-HFP): SPNs=90:10	3.101	0.08208	0.601
P(VDF-HFP): SPNs=85:15	2.825	0.16529	0.571
P(VDF-HFP): SPNs=80:20	2.622	1.82211	0.512

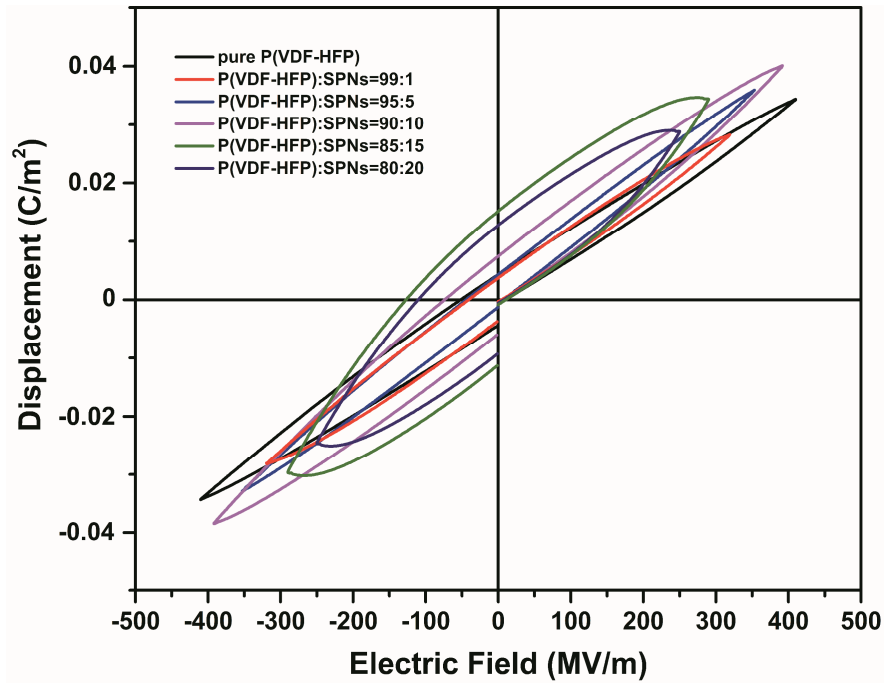


Fig. S6 D-E loops measured at 10 Hz and at room temperature for the pure P(VDF-HFP) and P(VDF-HFP)/SPNs nanocomposites.

Table. S3 Polarization, E_b and energy density of the pure P(VDF-HFP) and P(VDF-HFP)/SPNs nanocomposites derived from polarization against electric field loops.

Sample	Polarization/ C/m^2	E_b / MV/m	Energy density/ J/cm^3
pure P(VDF-HFP)	0.034	410	4.8
P(VDF-HFP): SPNs=99:1	0.028	320	3.1
P(VDF-HFP): SPNs=95:5	0.035	350	4.2
P(VDF-HFP): SPNs=90:10	0.039	390	5.1
P(VDF-HFP): SPNs=85:15	0.034	290	2.8
P(VDF-HFP): SPNs=80:20	0.028	250	1.9

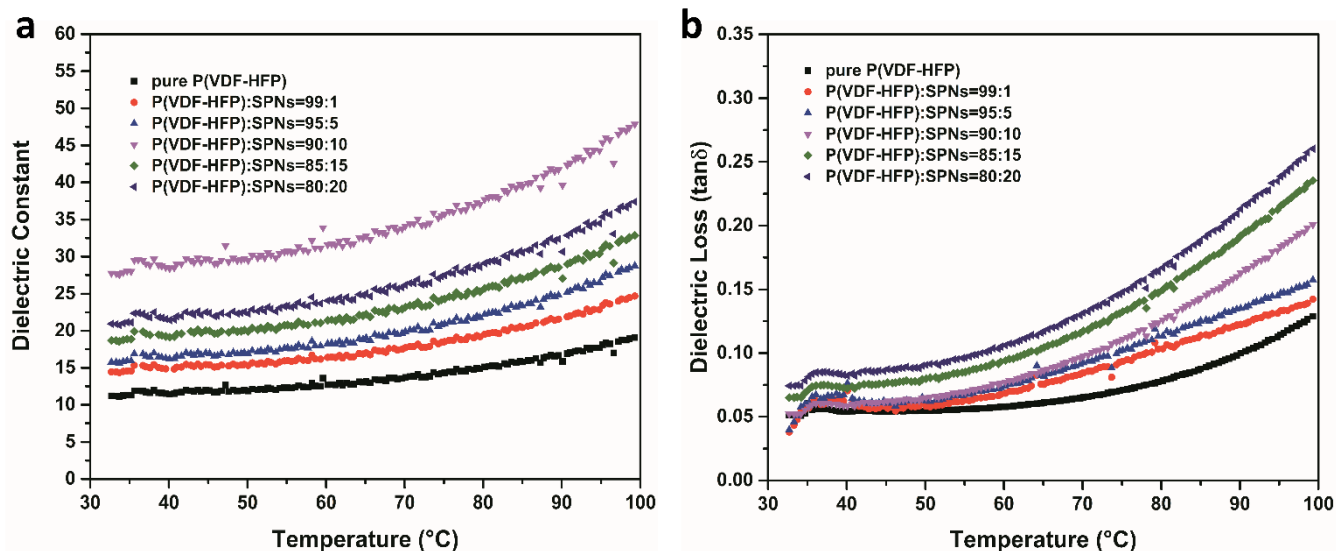


Fig. S7 Temperature dependence of a) dielectric constant and b) dielectric loss of pure P(VDF-HFP) and P(VDF-HFP)/SPNs nanocomposites with different SPNs contents.

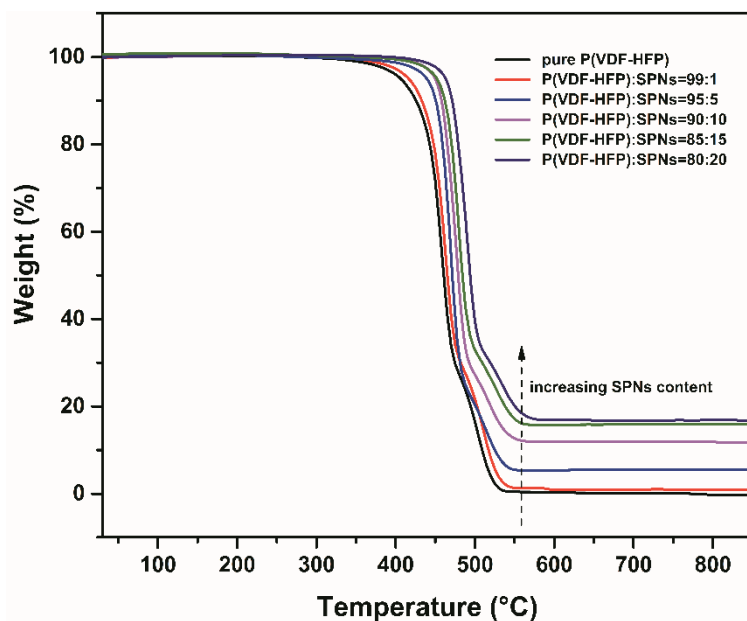


Fig. S8 TG curves of pure P(VDF-HFP) and P(VDF-HFP)/SPNs nanocomposites with different SPNs contents.

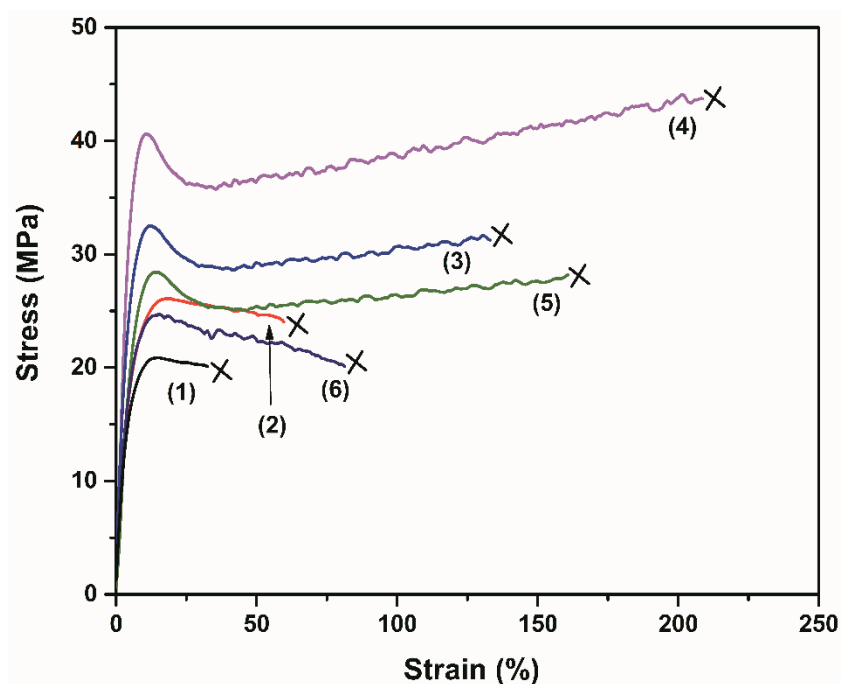


Fig. S9 Strain-stress curves of (1) pure P(VDF-HFP) and a series of P(VDF-HFP)/SPNs nanocomposite films with SPNs contents of (2) 1 wt.%, (3) 5 wt.%, (4) 10 wt.%, (5) 15 wt.% and (10) 20 wt.%.

Reference

1. K. Ma, U. Werner-Zwanziger, J. Zwanziger and U. Wiesner, *Chem. Mater.*, 2013, **25**, 677-691.
2. P. Martins, A. C. Lopes and S. Lanceros-Mendez, *Prog. Polym. Sci.*, 2014, **39**, 683-706.
3. L. Li, C. Y. Li, C. Ni, L. Rong and B. Hsiao, *Polymer*, 2007, **48**, 3452-3460.
4. M. C. García-Payo, M. Essalhi and M. Khayet, *J. Membrane. Sci.*, 2010, **347**, 209-219.
5. B. D. Cullity and S. R. Stock, *Prentice Hall*, 2001.
6. Lee J S, Shin K Y, Kim C and Jiang J, *Chem. Commun.*, 2013, **49**(94):11047-9.